analytical chemistry

Article

pubs.acs.org/ac

Automated Assignments of N- and O-Site Specific Glycosylation with Extensive Glycan Heterogeneity of Glycoprotein Mixtures

John S. Strum,[†] Charles C. Nwosu,[†] Serenus Hua,[†,‡] Scott R. Kronewitter,[†] Richard R. Seipert,[†] Robert J. Bachelor,[†] Hyun Joo An,[‡] and Carlito B. Lebrilla*[,†,§]

[†]Department of Chemistry, University of California, Davis, California 95616, United States

[‡]Graduate School of Analytical Science and Technology, Chungnam National University, Daejeon, South Korea

[§]Department of Biochemistry and Molecular Medicine, University of California, Davis, California 95616, United States

Supporting Information

ABSTRACT: Site-specific glycosylation (SSG) of glycoproteins remains a considerable challenge and limits further progress in the areas of proteomics and glycomics. Effective methods require new approaches in sample preparation, detection, and data analysis. While the field has advanced in sample preparation and detection, automated data analysis remains an important goal. A new bioinformatics approach implemented in software called GP Finder automatically distinguishes correct assignments from random matches and complements experimental techniques that are optimal for glycopeptides, including nonspecific proteolysis and high mass resolution liquid chromatography/tandem mass spectrometry (LC/MS/MS). SSG for multiple N- and O-glycosylation sites, including extensive glycan heterogeneity, was annotated for single proteins and protein mixtures with a 5% false-discovery rate, generating hundreds of nonrandom glycopeptide matches and demonstrating the proof-of-concept for a self-consistency scoring algorithm shown to be compliant with the target-decoy approach (TDA). The approach was further applied to a mixture of N-glycoproteins from unprocessed human milk and O-glycoproteins from very-low-density-lipoprotein (vLDL) particles.

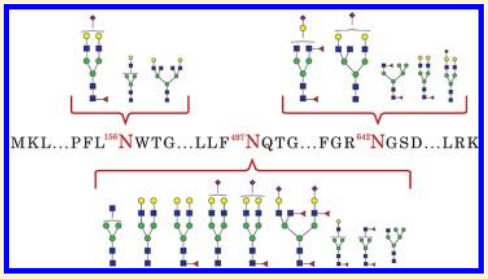

Characterizing glycoproteins through the determination of site-specific glycosylation (SSG) is one of the key analyses required for understanding glycoprotein functions. SSG describes the glycan heterogeneity for each occupied glycosylation site of a glycoprotein, including N- and O-glycosylation.[1] It has gained increased currency in the glycoproteomics[2] community, albeit little consensus regarding implementation.[3]

Determining SSG is complicated by microheterogeneity, which is the large number of glycans occupying a single site. The analysis is also complicated by difficulties associated with the mass spectrometry (MS) characterization of glycopeptides. The glycan component is composed of relatively few unique monosaccharides, several with identical masses, a fact that increases the redundancy and similarity of theoretical glycans among competing matches. Because glycopeptides often contain glycans with similar monosaccharide compositions, MS methods, even those capable of obtaining highly accurate masses, are insufficient. Tandem MS is often employed to obtain structural characterization; however, the presence of glycan isomers as well as the difficulty in obtaining comprehensive peptide and glycan fragmentation renders this method wholly insufficient.[4] Even if comprehensive fragmentation were available, glycopeptide analysis is still complicated by nonlinear glycan structures that often preclude monosaccharide sequencing with de novo[5] methods commonly used for peptides. For this reason, chromatographic separation is performed to separate isomeric glycopeptide species. The combination of accurate mass, tandem MS, and chromatographic separation provide comprehensive analysis if they can be performed routinely in a rapid, automated manner.

Despite these difficulties, the need for SSG is in high demand in fields as diverse as biomarker discovery and recombinant protein therapeutics (biologics).[6] SSG and other post-translational modifications (PTMs) can vary with disease state in the former and in batch-to-batch manufacturing of the latter.[7,8] A difference in glycosylation as simple as the presence of fucose can render a biologic ineffective or toxic, depending on the binding receptor of the target entity.[9] As patents end for biologics, the so-called biosimilars will be required by regulatory agencies to demonstrate similar PTMs if additional clinical trials demonstrating bioequivalence are to be minimized. Furthermore, industry and academia alike require tools capable of analyzing SSG within complex protein mixtures to understand protein behavior and function.[10,11] However, mixture analysis is problematic because the theoretical glycopeptide compositions from different glycoproteins are often quite similar. The recurring challenge in glycoproteomics is achieving distinction amidst similarity.

Received: September 25, 2012
Accepted: May 10, 2013
Published: May 10, 2013

   dx.doi.org/10.1021/ac4006556 | *Anal. Chem.* 2013, 85, 5666−5675

Common experimental techniques for the analysis of glycopeptides include hydrophilic interaction chromatography (HILIC)[12] and generation of diagnostic glycan oxonium ions by tandem MS.[13−15] Glycoproteomics has been further enhanced by techniques that address the unique characteristics of the glycoproteome,[16] such as online deglycosylation[17] and nonspecific proteolysis.[18] In addition to employing high mass accuracy and high mass resolution with such techniques as Fourier transform ion cyclotron resonance mass spectrometry (FTICR MS),[19] mass spectral techniques have been improved with glycopeptide-centric strategies, such as higher-energy collision dissociation-accurate mass-product-dependent electron transfer dissociation (HCD-PD-ETD).[20] Similar to structural elucidation with nuclear magnetic resonance (NMR), which often requires ^{1}H NMR, ^{13}C NMR, UV−vis, infrared (IR), MS, and other complementary techniques, MS-based glycoproteomics is gravitating toward multifaceted approaches using several parallel experiments. Such analyses combine reverse phase (RP) and HILIC chromatography for peptide- and glycan-centric separations as well collision-induced dissociation (CID), electron capture dissociation/electron transfer dissociation (ECD/ETD), specific and nonspecific proteolysis, glycan release (typically PNGase F), and dual polarity ionization.[21−23] An example of such an approach is in-gel nonspecific proteolysis for elucidating glycoproteins (INPEG).[23] Glycoproteomics has also benefitted from novel data analysis approaches such as limiting theoretical possibilities to biologically relevant libraries[24,25] and determining N-glycan topology from glycan family information.[26]

In addition to glycopeptide-tailored instrumentation and sample preparation, several valuable software tools are available to analyze SSG, although they have focused primarily on N-glycosylation.[27] Some tools, such as GlycoExtractor,[28] combine proteomics and glycomics as parallel analyses.[29] This strategy often reveals glycan heterogeneity without knowledge of site specificity.[30] Other tools are partially or entirely de novo,[31] requiring only the raw data of detected glycopeptides with no prior knowledge of the protein IDs, such as GlyPID,[32] a tool that has been used with targeted multipass experiments to achieve SSG of complex mixtures. Several tools have taken advantage of proteomics while still retaining the analysis of intact glycopeptides, including GlycoMaster,[33] GlyDB,[34] GlycoMiner,[35] GlycoSpectrumScan,[36] GlycoPeptideSearch,[37] ByOnic,[38] SimGlycan,[39] Peptoonist,[40] and GlycoPep grader.[41] Peptoonist allows the user to first identify the nonglycosylated peptides with the well-established X!Tandem[42] proteomics algorithm and then determine which of the remaining isotopic envelopes, i.e., those not identified as peptides, are potential glycopeptides based on an averagine[43] composition for glycopeptides. In addition to the isotopic distribution and accurate mass, tandem MS may be used to identify glycopeptides. Software called GlycoPep grader performs glycopeptide analysis of tandem MS data starting at the point where the user has generated a list of potential glycopeptide compositions. The online software uses an algorithm based on the predictable fragmentation for different categories of glycosylation. Another useful software tool was developed by Joenväärä et al.[44] that successfully identified 26 serum glycoproteins from 80 N-glycopeptides.

We have previously introduced a software tool named GlycoX[45] that yielded comprehensive SSG of single proteins. In contrast to contemporaneous software, GlycoX was equipped to deal with nonspecific protease digests, which contrasted to the widely used specific proteases such as trypsin. The use of tryptic digests and nonspecific proteases are complementary, each with unique advantages and disadvantages. Tryptic digests yield distinct and well-characterized cleavages that readily yield protein identification. However, because few peptides are glycosylated in nearly all proteins, the vast majority of the peptide products are not glycosylated. Nonglycosylated peptides ionize more effectively than the glycosylated ones, so that one or more glycopeptide enrichment steps are necessary for analysis.[46] Tryptic digestion may further produce missed cleavages particularly near the site of glycosylation yielding large glycopeptides that are not amenable using standard tandem MS methods.[31,47,48] Conversely, nonspecific proteases generate heterogeneous peptide products that split the detection of a particular glycosylation site among a family of related peptides. Identifying the glycopeptide is complicated by the lack of specificity. However, the method is effective at yielding enriched peptide products without extensive purification. In addition, it yields singly glycosylated peptides even when additional glycosylation sites are nearby.

A comprehensive solution for N- and O-glycopeptide analysis is provided to work with both specific and nonspecific protease digests.[18,49−55] A new software called GlycoPeptide Finder (GP Finder) is presented, which works independent of the type of enzyme and mass spectrometry platform. Rather than using data-reduction according to a specific enzyme, all possibilities are calculated to accommodate nonspecific proteases, such as Pronase E, which generates smaller glycopeptides. Glycans are observed with a peptide tag that identifies the protein and the glycosylation site. While the use of nonspecific proteases is more challenging for data interpretation because the sizes of the peptide tags are variable, sometimes too short for site determination, the variability can be controlled with the digestion time. The variable peptide lengths around the glycosylation sites correspond to multiple glycopeptides that can be used to provide self-consistency in the assignments.[18,50,53,54]

METHODS

Materials and Reagents. Pronase E proteases, cyanogen bromide (CNBr) activated sepharose 4B (S4B) beads, bovine pancreatic ribonuclease, bovine lactoferrin, bovine kappa casein, and bovine fetuin were obtained from Sigma Aldrich (St. Louis, MO). Graphitized carbon cartridges were purchased from Grace Davison Discovery Sciences (Deerfield, IL). All chemicals used were either of analytical grade or better.

Protease Digestion and Glycopeptide Cleanup. The site-specific glycosylation analysis workflow of the protein cocktail mixture has been previously described.[52] After digestion with Pronase, the samples were cleaned up with solid phase extraction (SPE) and collected as two fractions: 20 and 40% acetonitrile. The N-linked glycopeptides appeared primarily in the 20% fraction, whereas the O-linked were in the 40% fraction. For proof of concept we analyzed each fraction separately by data dependent LC/MS/MS; however, the combined data of the two LC/MS/MS runs were processed both separately and simultaneously as if obtained from a single chromatographic experiment. Therefore two fractions need not be collected and analyzed separately for the purposes of the software analysis.

Mass Spectrometry Analysis. Glycopeptide mixtures were analyzed using an Agilent 1200 series LC system coupled to an Agilent 6520 quadrupole-time-of-flight (Q-TOF) mass

dx.doi.org/10.1021/ac4006556 | Anal. Chem. 2013, 85, 5666−5675

spectrometer (Agilent Technologies, Santa Clara, CA). The HPLC-Chip/Q-TOF system was equipped with a micro well-plate autosampler (maintained at 6 °C by a thermostat), a capillary loading pump for sample enrichment, a nanopump as the analytical pump for sample separation, HPLC-Chip Cube, and the Agilent 6520 Q-TOF MS detector. The tandem mass spectra of the glycopeptides were acquired in a data-dependent manner following LC separation on the microfluidic chip. The microfluidic chip consisted of a 9 mm × 0.075 mm i.d. enrichment column and a 150 mm × 0.075 mm i.d. analytical column, both packed with 5 μm porous graphitized carbon (PGC) as the stationary phase. Glycopeptides were subjected to collision-induced fragmentation with nitrogen as the collision gas using a series of collision energies that were dependent on the m/z values of the different glycopeptides and peptides. The collision energies correspond to voltages ($V_{collision}$) that were based on the equation: $V_{collision} = m/z$ (1.8/100 Da) V − 2.4 V; where the slope and offset of the voltages were set at (1.8/100 Da) and (−2.4), respectively. The preferred charge states were set at 2, 3, >3, and unknown. Detailed experimental setup and instrumental parameters are provided in the previous publications by Nwosu et al.[23,52]

Data Processing. Prior to data analysis, each tandem spectrum was deconvoluted, deisotoped, and adjusted to neutral masses with commercially available software called MassHunter (Agilent Technologies, Santa Clara, CA). The mass list of the glycopeptide precursor ions was analyzed with our in-house software, GP Finder, for rapid SSG analysis. The GP Finder is a considerable improvement on the previously developed GlycoX,[45] offering several new features including glycan libraries with biological filters to reduce false-positive hits, support for protein mixture analysis and tandem MS, faster run-time, and a significantly improved user interface. All glycopeptide assignments were made within a specified tolerance level (≤20 ppm). Each glycopeptide identity was further verified by tandem MS for detailed structural information. The software and test data are available to download from http://chemgroups.ucdavis.edu/~lebrilla/GPF_docs.zip.

Candidate glycopeptide compositions were filtered according to the presence of diagnostic oxonium ions, accurate mass, and biological rules that are species-specific.[25] The tandem MS fragments were filtered by mass and biological rules. The best match for each spectrum was determined by GP Finder according to tandem MS data and self-consistency among the results (eq 1−4). The algorithms and workflow for GP Finder are provided with further discussion in the Supporting Information.

The N- and O-glycosylation sites can be determined in two ways: automatically by the software or manually by the user. Potential N-linked sites are automatically determined by the software by either the consensus sequence NXT or NXS (X is not proline) or the annotated sites that are included in the reviewed sequence entries in the UniProt Knowledgebase. O-linked sites are determined by a number of methods, the most efficient of which is to use annotated UniProt entries. Unfortunately, Q-TOF CID cannot always localize O-glycosylation and the Pronase approach may fail on mucin-type O-glycosylation in which there are multiple glycosylation sites separated by only a few residues.[56] Although O-linked sites can be specified by the user, their determination is a confirmation rather than a characterization when based solely on UniProt entries.[57]

Two decoy generation strategies were investigated, both using the actual protein sequences as well as the actual experimental masses. The first strategy, a more traditional method, shuffled the amino acids of the known proteins with a standard (nearly random) Java algorithm, conserving the glycosylation sites and consensus sequences yet resulting in poor modeling. The second strategy did not shuffle the sequences; instead an 11-Da residue was added as part of each theoretical glycan composition, preserving the true peptide sequences around each site and providing a better model for the random matches to the highly weighted peptide (P) and peptide + HexNAc (PN) peaks. The latter was employed with GP Finder. The decoy data sets were created with 11-Da artificial components to prevent the randomly generated glycan compositions from matching glycans that could actually be present in the sample. The 11-Da residue is small enough that the remaining portion of the glycan composition is comparable in size to the glycan compositions in the target data set and unique enough that we do not expect it to appear in any compounds of interest. The use of 11 Da also avoids the pitfall of numbers such as 1, 12, 14, 15, 16, and 18 Da, that could be confused with common organic components.

For the data set-bias test, the target and decoy libraries compete for top scoring matches to fabricated, incorrect tandem data that have been generated from the actual tandem spectra by adding 11-Da to all peaks in the tandem spectra.[58] The adjusted tandem spectra are used for determining whether a set of false tandem spectra will match equivalently to both decoy and target glycopeptide compositions. While it is true that both the false tandem spectra and the decoy glycopeptide compositions use 11-Da, they do not generate matches that are systematically related to 11-Da because the 11-Da component is not included in the composition of the decoy glycopeptides when comparing their in silico fragments to tandem data. Furthermore, the 11-Da component is subtracted once from each experimental precursor mass; whereas, it is added to each of the tandem fragment masses, thus preventing the possibility that a precursor mass and a fragment mass are both adjusted by 11-Da in the same way.

Scores are generated in three distinct phases. First, a Base Score is generated (eq 1), followed by a boost in score from self-consistency in the data (eq 2) and then subsequent compensation for target-decoy Bias (eqs 3 and 4). The Base Score is calculated according to the number of fragments observed for each fragment type for a particular theoretical glycopeptide and according to the user-defined weight given to each type of fragment (eq 1). The weights applied here were based on the relative importance that we predicted for each fragment type. The Boosted Score for each glycopeptide is calculated in two steps (eq 2). The number of unique glycopeptide masses in each peptide family is multiplied by a user-defined weight (we used 1) and then added to the associated Base Score as a temporary adjustment. The average adjusted score for each peptide family from the set of adjusted Base Score values (referred to as the Family Average) is then calculated and added to each associated Base Score (original, nonadjusted value).

A Bias in the target data set relative to the decoy data set results from applying self-consistency scoring. Prior to estimating the Bias, GP Finder first calculates the average size of all the decoy peptide families and the average Boosted Score for the entire decoy data set (referred to as the Average Boosted Decoy Score). Second, a representative score of

dx.doi.org/10.1021/ac4006556 | Anal. Chem. 2013, 85, 5666−5675

random self-consistency in the target data set is obtained by determining the average Boosted Score from all target matches that have a peptide family size equal to the average decoy peptide family size (referred to as the Average Subset Boosted Target Score). The most conservative estimation of the Bias is to subtract the Average Boosted Decoy Score from the Average Subset Boosted Target Score (eq 3). The Final Score is calculated by subtracting the Bias from each Boosted Score (eq 4).

$$\text{Base Score} = 5 \times (\text{P} + \text{PN})^2 + 4 \times (\text{b/y}) + 3 \times (\text{B/Y}) + 2 \times (\text{gp}) + 1 \times (\text{glycan}) \quad (1)$$

where the counts for each fragment type are represented by the following: P = intact peptide, PN = intact peptide + HexNAc, b/y = b and y peptide-only fragments, B/Y = b and y glycopeptide fragments with intact peptide, gp = glycopeptides fragmented on glycan and peptide, and glycan = glycan-only fragments.

$$\text{Boosted Score} = \text{Base score} + \text{Family Average} \quad (2)$$

$$\text{Bias} = \text{Average Subset Boosted Target Score} - \text{Average Boosted Decoy Score} \quad (3)$$

$$\text{Final Score} = \text{Boosted Score} - \text{Bias} \quad (4)$$

The approach performs similarly to specific digestion with QTOF MS/MS, although below what can be done with HCD/ETD combined with high mass accuracy. For this reason, we previously developed a sample preparation method called INPEG[23] that enriches for both glycoproteins and glycopeptides without cleanup steps between handling the unprocessed sample and analyzing with LC/MS/MS. INPEG also separates mixtures into less complex subsets that are appropriate for this bioinformatics approach. Furthermore, employing INPEG or some other protein identification strategy is required for GP Finder.[23]

Although not yet tested, the scoring scheme as implemented here is not likely to work for ETD because it relies heavily on P and PN; however, these parameters can be changed by the user to emphasize peptide backbone fragmentation. To some extent the self-consistency algorithm regains the sensitivity and specificity lost from the nonspecific digest.

RESULTS AND DISCUSSION

Experimental and Data Analysis Workflow. An outline of the method is shown in Figure S-1 in the Supporting Information. Digestion of the glycoprotein mixture was followed by solid phase enrichment to yield primarily glycopeptides that were analyzed by nanoflow LC/MS/MS. A large number of spectra were obtained with the vast majority corresponding to glycopeptides (for example, 60% of the nearly 1700 tandem spectra collected for human milk whey and vLDL contained one or more of the diagnostic oxonium ions within a tolerance of $m/z \pm 0.05$). To separate glycopeptide spectra from random, uninformative ones, a number of diagnostic peaks from tandem MS were used, such as the fragments corresponding to the peptide (P) and peptide + HexNAc (PN or more commonly Y_1).

For each sample reported here, a histogram demonstrated the bimodal distribution of scores, which was shown to distinguish the correct matches for previously annotated control samples. The histograms in Figure 1 were populated by the top scores from all tandem spectra of a control mixture. The overlap between the decoy and target score distributions allowed estimation of the false discovery rate (FDR).[59]

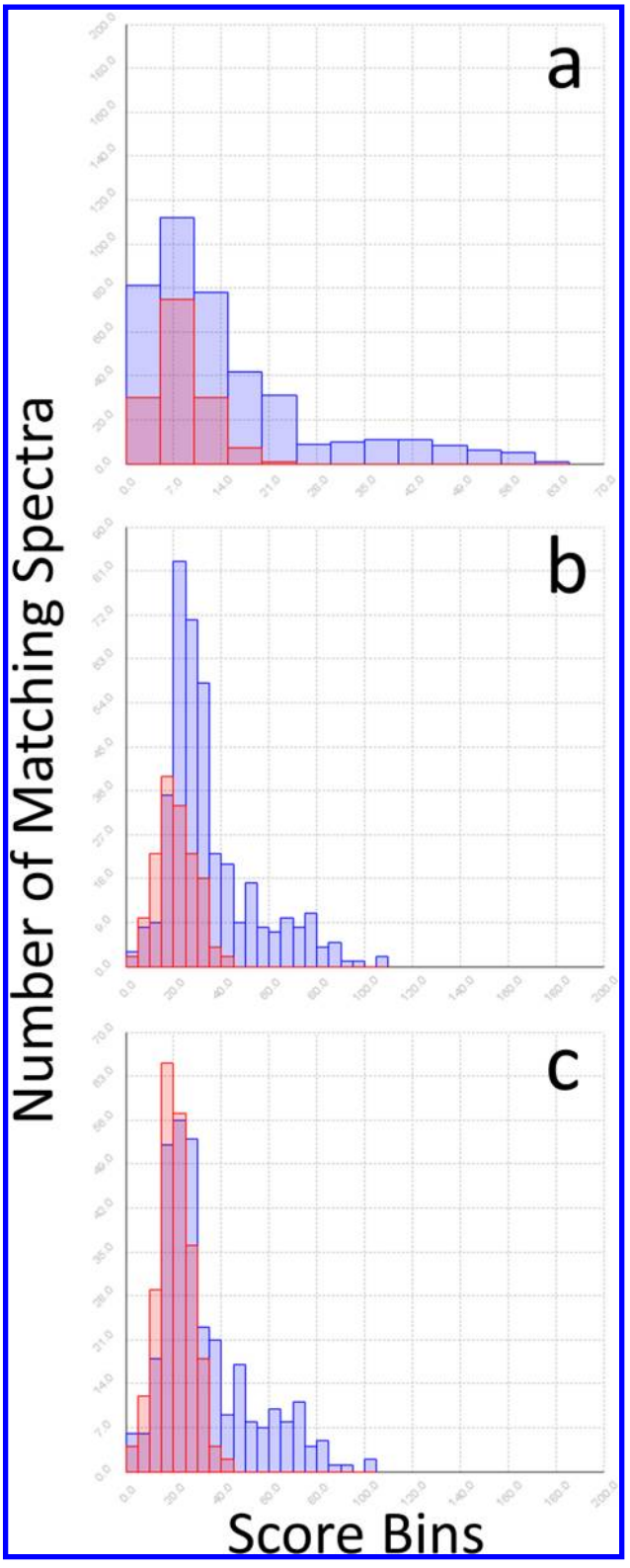

Figure 1. TDA compliance: score distributions of the target and decoy N-glycopeptide matches from the mixture of bovine fetuin, lactoferrin, and kappa casein. Data includes both 20 and 40% ACN SPE fractions: (a) without self-consistency, (b) with self-consistency, and (c) with self-consistency and TDA-compliance.

dx.doi.org/10.1021/ac4006556 | Anal. Chem. 2013, 85, 5666−5675

Scoring. An abundance of mass peaks and theoretical matches to all types of fragments requires us to balance the influence of the unique versus common pieces of evidence. Unbalanced weighting of scores leads to either artificially separated target-decoy populations or entirely overlapping ones (Figure S-2 in the Supporting Information). The algorithm effectively uses both common and unique fragments to identify the best matches in a systematic way that often cannot be duplicated by evaluating each spectrum manually.

Prior to examining the test data, we predicted the relative importance of each type of fragment that could be generated from an intact glycopeptide precursor ion.[60] Predictions were based on widely observed diagnostic fragments that are characteristic within a broad range of collision energies.[38,44,61−63]

The P and PN fragments are frequently observed for glycopeptides and are particularly rare for incorrect matches because of the unique amino acid composition required for the intact peptide. The b and y peptide fragments are somewhat unique and therefore also rare for incorrect matches with the exception of some overlap between peptide sequences common among both target and decoy matches. Unfortunately, the extent of peptide fragmentation with collision induced dissociation (CID) is attenuated for glycopeptides because the glycosidic bonds are labile and the fragmentation process is stochastic. Another important set of diagnostic peaks are the glycopeptide fragments containing a fragmented glycan and an intact peptide (B and Y ions); however, a few false matches to these peaks are somewhat common. While testing this scoring scheme, we monitored data that had been previously annotated. We found that even in the rare cases when a random false match had both P and PN, if the assigned fragments did not distinguish them (Figure S-3 in the Supporting Information), the self-consistency did.

Unfortunately, the parameters of mass deconvolution can favor some of these fragment types over others. For this reason, we employed commercial mass deconvolution software prior to input into GP Finder that assumes peptide molecular composition and identifies all the peptide fragments at the expense of a few glycopeptide fragments (Figures S-4 and S-5 in the Supporting Information). The glycan-only fragments were readily identified and useful for filtering out poor matches; however, similar glycosylation among theoretical matches is common, making glycan-only fragments poor differentiators between two or more seemingly good matches (except when a pair of peaks is detected for NeuAc and NeuAc-H_2O, eliminating all nonsialylated possibilities). Some fragment types are ignored to reduce random matches, including internal peptides and certain rearrangements (Figures S-6 and S-7 in the Supporting Information), leaving some peaks unassigned.

The extent of random matches is modeled by a decoy data set that competes with target data for the highest scoring match to each tandem spectrum. If the scoring method truly favors correct assignments and if sufficient data points are collected, the histogram of all the top scores for the target data should include two distributions, matches with considerable evidence (presumably correct) and random matches (presumably incorrect).[59] The decoy distribution should model the random matches and overlap with the lower-scoring population of target matches. By calculating the percent overlap between the decoy and the high-scoring target population, the false discovery rate (FDR) is estimated.

Target-Decoy Approach and Self-Consistency. A data set-bias test provides evidence that the decoy data set correctly models the target data.[58] As shown in Figure S-8 in the Supporting Information, the decoy and target data sets generated a similar shape and frequency of matches to incorrect tandem spectra. While a successful test is not proof of correct modeling, a failed test is proof of incorrect modeling.

The decoy data set was included with the target data during the analysis of real tandem data and competed with the target data (Figure 1a). The decoy distribution modeled the shape of the low scoring target matches well; however, the heights were not the same. On the basis of the data set-bias test, we expected the intensities to be similar. The inconsistency indicated either that the decoy data did not correctly model the incorrect matches in the target data or that the low scoring target data included some correct assignments.

We extracted potentially correct target matches out of the low scoring distribution by applying a self-consistency scoring algorithm (Figure 1b). The self-consistency algorithm identified families[50,52] of peptide heterogeneity. Unlike tryptic digestion that provides only glycan-based self-consistency, as described by Goldberg et al.,[38] Pronase digestion generates peptide-based self-consistency. Each glycan is expected to be detected on multiple glycopeptides with different peptide tag lengths around the same glycosylation site. The self-consistency described here provides more than an occasional opportunistic boost in score, as described by Gupta et al.[64] for the common double-pass filters that are used for boosting scores of neighboring peptides detected from a given protein; in contrast, the self-consistency in Pronase digestion is consistently observed[50,52] and is empirically indicative of correct assignments (Table S-1 in the Supporting Information). We tested several variations of these steps, as shown in Figure S-2 in the Supporting Information.

Recent candid discussion in the field[64,65] benefited our analysis by drawing our attention to the requirements for rigorous TDA-compliant analysis. The generally accepted premise of TDA is that the "matches to decoy peptide sequences and false matches to sequences from the original database follow the same distribution."[66] The timely discussion showed us that the random self-consistency in the target data will necessarily gain an advantage over the random self-consistency in the decoy data. Assuming the target data contains at least some correct matches to the tandem spectra, the target data will naturally have more high-scoring correct matches than the decoy. The boost in score for the incorrect (random) target matches as a result of self-consistency with correct target matches is therefore not accounted for in the decoy data. While some random incorrect target matches gain a boost in score and are included in the results, an even more abundant population of correct matches is boosted under these conditions. Furthermore, the average boost in score that is caused by random matches in the target data can be determined and removed as shown in Figure 1c where the decoy and low-scoring target distributions are similar in shape and height after employing the TDA-compliant self-consistency algorithm.

The self-consistency scoring presents an unknown factor: the ratio of correct to incorrect matches that have been boosted within the target data. We have accounted for this bias by calculating the difference between the random score boost for the target and decoy data. The algorithm is discussed in detail in the Methods section and is provided in the Supporting Information.

dx.doi.org/10.1021/ac4006556 | *Anal. Chem.* 2013, 85, 5666−5675

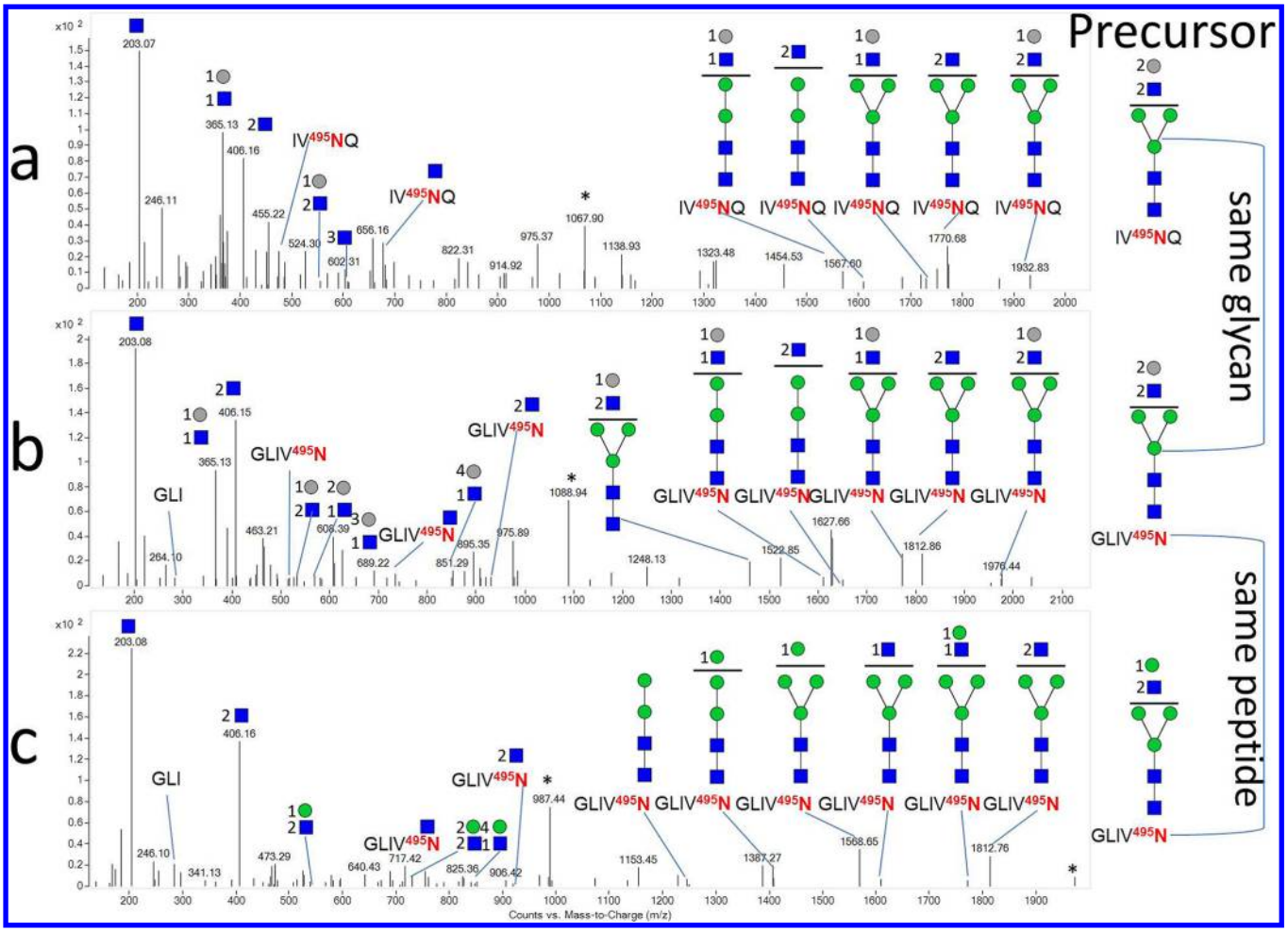

Figure 2. Self-consistent data: Tandem mass spectra of site-specific N-glycopeptide analysis at site 495 of bovine lactoferrin (TRFL) showing putative glycan structures. Glycan self-consistency is shown in parts a (m/z 1068.9363) and b (m/z 1089.9696). Peptide self-consistency is shown in parts b and c (m/z 988.4189). Blue squares, HexNAc; gray circles, Hex; green circles, Man; ∗ denotes precursor.

Table 1. Score Components for Data in Figure 2 and Figure S-10 in the Supporting Information as Computed by Equations 1−4

		scores					fragment counts					
glycopeptide	protein	final	base	fam. aver.	bias	fam. size	P	PN	b/y	B/Y	gp	glycan
IV^{495}NQ 4 Hexose 5 HexNAc	TRFL	67	43	29	5	12	1	1	0	6	0	5
GLIV^{495}N 4 Hexose 5 HexNAc	TRFL	74	50	29	5	12	1	1	1	6	0	8
GLIV^{495}N 4 Hexose 4 HexNAc	TRFL	60	35	30	5	14	0	1	1	7	0	5
SGEP^{152}TS^{154}TPT Hex HexNAc 2 NeuAc	CASK	86	49	40	3	22	1	1	3	3	0	8
GEP^{152}TS^{154}TPT Hex HexNAc 2 NeuAc	CASK	95	58	40	3	22	1	1	4	4	0	10
GEP^{152}TS^{154}TPT Hex HexNAc NeuAc	CASK	69	43	29	3	10	1	1	3	2	0	5

Figure 2 shows the self-consistency among three spectra for N-glycopeptides with the same glycosylation site. The top two fragmentation spectra are related by having the same glycan composition but different peptide, for which both spectra show the presence of P, Hex:HexNAc, and several related Y glycopeptide fragments. The bottom two fragmentation spectra have a common peptide but different yet related glycans. The resultant fragmentation data both exhibit the presence of the PN + HexNAc and b_3 peptide ions. All three spectra contain fragments of PN and 2HexNAc. The components of the scores are provided in Table 1. Additional spectra showing SSG, including O-linked examples, are provided in Figures S-5 and S-9 in the Supporting Information.

O-glycosylation can be challenging to match confidently, even though it consistently generates more extensive peptide fragmentation than N-glycosylation. The challenge is due to the lack of a consensus sequence coupled with the high occurrence of serine and threonine residues around O-glyosylation sites. For instance, the candidate glycopeptides for the spectra shown in Figure S-10 in the Supporting Information could be glycosylated on either of the two glycosylation sites on the same peptide, making these results site-directed as opposed to site-specific. Site-directed results for these spectra distinguish glycan heterogeneity at sites 152 and 154 from the surrounding sites: 142, 157, 163, and 186, as shown in Table 1. Without self-consistency the scores for sites 152 and 154 are equal, even though there is some ambiguity with site 152 because the data

dx.doi.org/10.1021/ac4006556 | Anal. Chem. 2013, 85, 5666−5675

lacks the y_3 and y_4 peptide ions that may be more likely to be observed with glycosylation on site 152 (coincidentally, the y_4 peptide ion is observed in a potentially isomeric compound that eluted 7 min earlier than the data shown in Figure S-10 in the Supporting Information). Furthermore, the peptide heterogeneity shows proteolytic cleavage at several sites C-terminal to 154 yet does not show cleavage of residues 153 or 154 C-terminal to 152. However, we cannot yet make conclusions from the lack of data in a particular spectrum or peptide family. Nonetheless the two possibilities are slightly different using self-consistency scoring. It is also unclear at this point how much bias is imposed on site 154 from its simultaneous proximity to both sites 152 and 157. For this reason, as well as the fact that few false matches are available for plotting populations of random false matches per spectrum, the results are not claimed to be inherently correct, rather they are a pragmatic way of comparing and presenting the evidence.

Some degree of qualitative legitimacy is demonstrated by analyzing tandem MS data with an intentionally low or high mass tolerance for the method, such as 5 ppm and 1 Da. The result is that the decoy and target distributions are not separated; however, the distributions are in fact separated with an appropriate mass tolerance for the method, such as 80 ppm. The correct mass tolerance window is an effective sweet-spot that distinguishes correct self-consistency scoring from random self-consistency.

Analysis of Single Protein with One Site of Glycosylation. We analyzed a glycoprotein with well-characterized glycosylation: bovine pancreatic ribonuclease (RNaseB). As part of the in silico digest for the analysis of RNaseB, we also included the sequences from a three-protein mixture to probe the actual FDR. That the method is superior to manual analysis is illustrated in this application. Manual analysis, previously performed on this data by an experienced analyst, yielded 26 glycopeptides, all of which were also selected by GP Finder as the top possibilities for their respective spectra (Table S-2 in the Supporting Information). GP Finder identified 18 additional RNaseB glycopeptides that scored within the 5% FDR. Although the number of data points precludes a solid statistical analysis, the separation of the decoy and target matches was characteristic of data that we consider to be high quality (Figure S-11 in the Supporting Information). Manual analysis revealed that the true FDR at the threshold indicated by the 5% target-decoy overlap was 17%. The true 5% FDR threshold was a few points higher than the value calculated with TDA, encompassing 46 rather than 58 matches. The discrepancy was not surprising because the data set was small, with less certainty regarding the true shape of the decoy distribution in the decaying region of the histogram. The discrepancy may also be caused by our pragmatic method for calculating the target-decoy bias, for which the average random match will be corrected, while some subset of matches will either be over- or under-corrected.

Analysis of Three-Protein Mixture Each with Multiple Sites of Glycosylation. A protein mixture composed of bovine fetuin, lactoferrin, and kappa casein was created to serve as a substantially more difficult problem with 18 sites of N- and O-glycosylation. The height of the decoy distribution modeled the low-scoring target distribution considerably better after employing the TDA-compliant self-consistency algorithm, providing greater confidence in the assignments (Figure 1c). The total number of target N-glycopeptide matches above the 5% FDR was 106 without self-consistency, 133 with self-consistency, and 78 with the TDA-compliant self-consistency analysis (Tables S-3 and S-4 in the Supporting Information). Some matches were ambiguous because they included multiple top score possibilities for a single tandem mass spectrum and generally lacked sufficient peptide fragmentation to differentiate the possibilities. The inclusion of the RNaseB sequence (not actually present in the sample) generated one false match that scored just over the actual 5% FDR threshold. Although only peptide self-consistency was used to determine each glycoform, glycan self-consistency emerged from the results, as did heterogeneity of glycan types, such as the complex/hybrid and high mannose glycoforms observed on bovine lactoferrin site 495 (Figure 2 and Figure S-5 in the Supporting Information).

The O-linked matches behaved similarly to the N-linked ones, with increased separation between the correct and incorrect assignments after applying the self-consistency algorithm. The total number of target O-glycopeptides above the 5% FDR was 92 without self-consistency, 115 with self-consistency, and 61 with the TDA-compliant self-consistency analysis (Tables S-3 and S-4 in the Supporting Information). Additional validity is shown by comparing the results with an analysis considering only one of the O-linked glycoproteins present in the sample. While the empirically determined 5% FDR did not change between the two analyses, the size of the high-scoring population did change from 36 to 61 when both O-glycoproteins were included in the analysis (Figure S-12 in the Supporting Information).

Another source of ambiguity was the overlap among spectra assigned to both N- and O-linked glycopeptides. After comparing the separately analyzed N and O matches (generated from the same tandem MS data), 5% of the TDA-compliant results were false as a result of the overlap and required manual interpretation (Figure S-3 in the Supporting Information).

A second technique for calculating FDR corroborates the results obtained with the target-decoy approach and provides additional discovery rate statistics. By entering the heights of the histogram bars for the target data set from Figure 1c and Figure S-12b in the Supporting Information into a commercial peak deconvolution software (PeakFit[67]), the underlying distributions of the target data set were calculated (Figure S-13 in the Supporting Information) and used to estimate the FDR, false-negative rate (FNR), and accuracy.[59,68] The respective values for the N-linked analysis are 8.7%, <0.0%, and 98.4%. The values for the O-linked analysis are 10.4%, 14.9%, and 97.0%.

Analysis of Unknown Protein Mixtures. We applied the method to a mixture of glycoproteins from human very-low-density-lipoprotein (vLDL) nanoparticles. Tryptic analysis identified two O-glycoproteins, apolipoprotein C-III (APOC3, P02656), and apolipoprotein E (APOE, P02649) as well as apolipoprotein B (APOB, P04114), an N-glycoprotein. GP Finder identified 11 glycopeptides with high confidence (completely outside the decoy distribution) for APOC3 and APOE (SSG maps provided in Figure 3 and score histograms in Figure S-14 in the Supporting Information), for which the TDA-compliant self-consistency scoring draws a clearer distinction between the 11 high-scoring matches and the low scoring matches. Both O-glycoproteins were glycosylated on the sites that were annotated in the UniProt flat file. The confident assignments were associated with excellent tandem

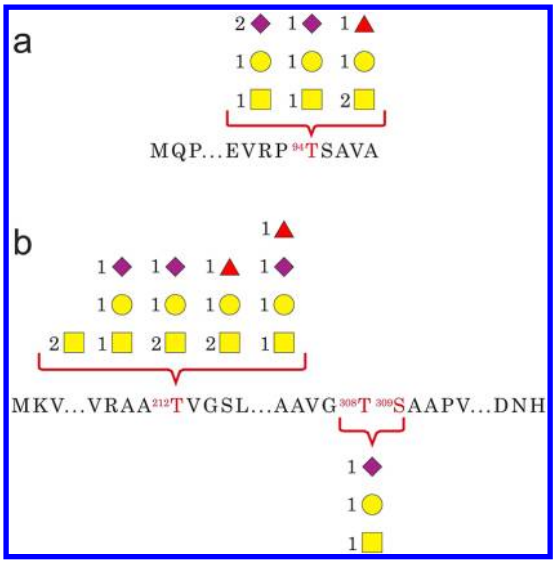

Figure 3. SSG map of O-glycoproteins: SSG of a mixture of proteins extracted from vLDL nanoparticles for two O-glycoproteins (a) APOC3 and (b) APOE. Yellow squares, HexNAc; yellow circles, Hex; purple diamonds, NeuAc; red triangles, dHex.

spectra that were also verified manually (Figure S-15 in the Supporting Information).

SSG was also analyzed for a refined pool of electrophoretically separated glycoproteins from raw human milk using the recently published INPEG method (Figure S-16 in the Supporting Information). The analysis included concurrent digests from parallel gel bands with nonspecific proteases and trypsin, providing separate glycopeptide-rich and tryptic peptide-rich samples for each band of refined human milk glycoproteins. Following digestion of the refined milk pool, the sample was separated and detected online with LC/MS/MS (Figure 4), reducing ion-suppression and revealing site-specific heterogeneity (SSG maps provided in Figures S-17 and S-18 in the Supporting Information). Two glycoproteins were identified from one band, lactoferrin (TRFL_HUMAN, P02788) and polymeric immunoglobulin receptor (PIGR_HUMAN, P01833), resulting in 22 and 58 glycopeptide assignments at a 5% FDR (histogram provided in Figure S-19 in the Supporting Information) covering 3 and 6 glycosylation sites, respectively.

CONCLUSION

An ideal scoring scheme generates separate populations of correct and incorrect matches after plotting all top scores in a histogram according to the frequency of scores within certain score bins. Diagnostic fragment types are awarded more significance than others. Two control samples demonstrate that the weighting factors applied here favor correct matches over incorrect ones for the described experimental conditions.

The method relies on the assumption that the decoy data set correctly models the random false matches in the target data.[69] Although we probe the validity of this assumption by analyzing previously annotated data sets, performing data set-bias tests and plotting the score distributions, we have relied on the FDR more as an effective means to filter out poor target matches than as a precise calculator for FDR. The validity of the FDR approximation is strengthened by our observation that poor tandem MS data does not produce target scores that are distinguishable from random decoy scores.

The final result is an automated and confident annotation of the site-specific or site-directed heterogeneity of every glycoprotein in the control mixture (Table S-4 in the

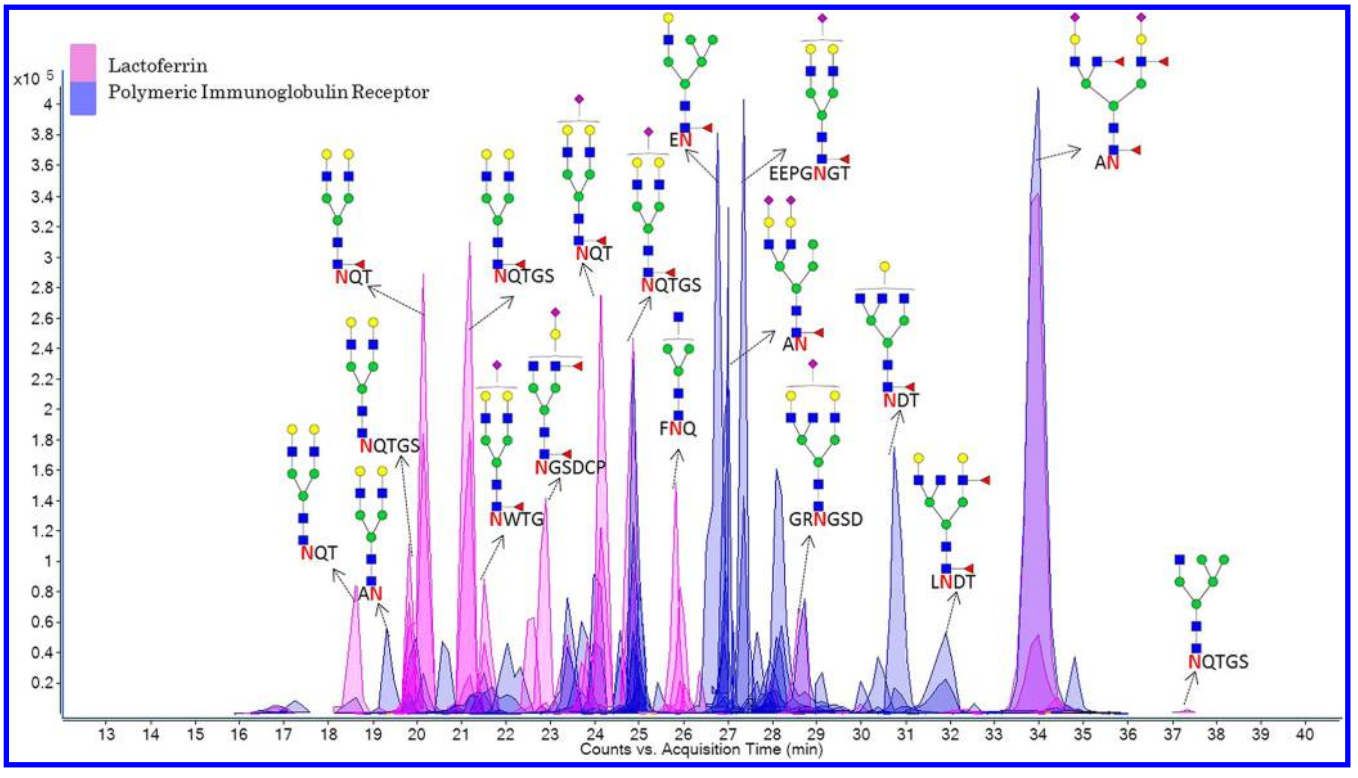

Figure 4. Separation of glycopeptides: online separation and detection of glycopeptides from human lactoferrin and polymeric immunoglobulin receptor, two glycoproteins isolated in a gel band after SDS-PAGE of raw human milk.

dx.doi.org/10.1021/ac4006556 | *Anal. Chem.* 2013, 85, 5666−5675

Supporting Information). While the self-consistency of peptides around each site is both expected and useful, the algorithm does not require a nonspecific protease and could potentially benefit from data reduction with specific proteases. This analysis is a step toward automated glycoproteomics, taking advantage of the power behind protein identification with shot-gun proteomics[66,70] and the specificity of a glycopeptide-optimized mixture analysis method. The method has been demonstrated on unknown glycoprotein mixtures from vLDL nanoparticles and human milk and has identified glycopeptides with score distributions that distinguish confident from random assignments.

■ ASSOCIATED CONTENT

Supporting Information

Additional information as noted in text. This material is available free of charge via the Internet at http://pubs.acs.org.

■ AUTHOR INFORMATION

Corresponding Author

*E-mail: cblebrilla@ucdavis.edu. Phone: +1-530-752-0504. Fax: +1-530-752-8995.

Notes

The authors declare no competing financial interest.

■ ACKNOWLEDGMENTS

We would like to thank Agilent Technologies for their contributions. Financial support was provided by the National Institutes of Health (Grant RO1GM049077 for C. B. Lebrilla) and the Korean Converging Research Center Program through the Ministry of Education, Science and Technology (Grant 2011K000968 for H. J. An). The table of contents graphic and Figure 3 were prepared by Rachel Strum.

■ REFERENCES

(1) Kolarich, D.; Jensen, P. H.; Altmann, F.; Packer, N. H. *Nat. Protoc.* **2012**, *7*, 1285−98.
(2) Pan, S.; Chen, R.; Aebersold, R.; Brentnall, T. A. *Mol. Cell. Proteomics* **2011**, *10*, R110.003251.
(3) Doerr, A. *Nat. Methods* **2012**, *9*, 36−36.
(4) Wuhrer, M.; Catalina, M. I.; Deelder, A. M.; Hokke, C. H. *J. Chromatogr., B: Anal. Technol. Biomed. Life Sci.* **2007**, *849*, 115−128.
(5) Hughes, C.; Ma, B.; Lajoie, G. A. *Methods Mol. Biol.* **2010**, *604*, 105−21.
(6) Walsh, G.; Jefferis, R. *Nat. Biotechnol.* **2006**, *24*, 1241−52.
(7) Butler, M. *Cytotechnology* **2006**, *50*, 57−76.
(8) Li, Y.; et al. *Anal. Chem.* **2011**, *83*, 240−245.
(9) Peipp, M.; et al. *Blood* **2008**, *112*, 2390−2399.
(10) Jenkins, N.; Parekh, R. B.; James, D. C. *Nat. Biotechnol.* **1996**, *14*, 975−981.
(11) Dove, A. *Nat. Biotechnol.* **2001**, *19*, 913−917.
(12) Alpert, A. J. *J. Chromatogr.* **1990**, *499*, 177−196.
(13) Sullivan, B.; Addona, T. A.; Carr, S. A. *Anal. Chem.* **2004**, *76*, 3112−3118.
(14) Demelbauer, U. M.; Zehl, M.; Plematl, A.; Allmaier, G.; Rizzi, A. *Rapid Commun. Mass Spectrom.* **2004**, *18*, 1575−1582.
(15) Dalpathado, D. S.; Desaire, H. *Analyst* **2008**, *133*, 731−738.
(16) Sun, B.; et al. *Mol Cell Proteomics* **2007**, *6*, 141−149.
(17) Qu, Y.; et al. *Anal. Chem.* **2011**, *83*, 7457−7463.
(18) Dodds, E. D.; Seipert, R. R.; Clowers, B. H.; German, J. B.; Lebrilla, C. B. *J. Proteome Res.* **2009**, *8*, 502−512.
(19) Wang, X.; Emmett, M. R.; Marshall, A. G. *Anal. Chem.* **2010**, *82*, 6542−6548.
(20) Saba, J.; Dutta, S.; Hemenway, E.; Viner, R. *Int. J. Proteomics* **2012**, *2012*, 560391.
(21) Leymarie, N.; Zaia, J. *Anal. Chem.* **2012**, *84*, 3040−3048.
(22) Deguchi, K.; et al. *Rapid Commun. Mass Spectrom.* **2006**, *20*, 741−746.
(23) Nwosu, C. C.; et al. *Anal. Chem.* **2013**, *85*, 956−963.
(24) Go, E. P.; et al. *Anal. Chem.* **2007**, *79*, 1708−1713.
(25) Kronewitter, S. R.; et al. *Proteomics* **2009**, *9*, 2986−2994.
(26) Goldberg, D.; Bern, M.; North, S. J.; Haslam, S. M.; Dell, A. *Bioinformatics* **2009**, *25*, 365−371.
(27) Dallas, D. C.; Martin, W. F.; Hua, S.; German, J. B. *Brief. Bioinform.* **2012**, DOI: 10.1093/bib/bbs045.
(28) Artemenko, N. V.; Campbell, M. P.; Rudd, P. M. *J. Proteome Res.* **2010**, *9*, 2037−2041.
(29) Tang, H.; Mechref, Y.; Novotny, M. V. *Bioinformatics* **2005**, *21* (Suppl 1), i431−i439.
(30) Geyer, H.; Geyer, R. *Biochim. Biophys. Acta* **2006**, *1764*, 1853−1869.
(31) Peltoniemi, H.; Joenvaara, S.; Renkonen, R. *Glycobiology* **2009**, *19*, 707−714.
(32) Wu, Y.; et al. *Rapid Commun. Mass Spectrom.* **2010**, *24*, 965−972.
(33) Xin, L.; Shan, P. *J. Biomol. Tech.* **2011**, *22*, S51−S52.
(34) Ren, J. M.; Rejtar, T.; Li, L.; Karger, B. L. *J. Proteome Res.* **2007**, *6*, 3162−3173.
(35) Ozohanics, O.; et al. *Rapid Commun. Mass Spectrom.* **2008**, *22*, 3245−3254.
(36) Deshpande, N.; Jensen, P. H.; Packer, N. H.; Kolarich, D. *J. Proteome Res.* **2010**, *9*, 1063−1075.
(37) Pompach, P.; Chandler, K. B.; Lan, R.; Edwards, N.; Goldman, R. *J. Proteome Res.* **2012**, *11*, 1728−1740.
(38) Bern, M.; Cai, Y.; Goldberg, D. *Anal. Chem.* **2007**, *79*, 1393−1400.
(39) Apte, A.; Meitei, N. S. *Methods Mol. Biol.* **2010**, *600*, 269−281.
(40) Goldberg, D.; et al. *J. Proteome Res* **2007**, *6*, 3995−4005.
(41) Woodin, C. L.; et al. *Anal. Chem.* **2012**, *84*, 4821−4829.
(42) Fenyö, D.; Beavis, R. C. *Anal. Chem.* **2003**, *75*, 768−774.
(43) Senko, M. W.; Beu, S. C.; McLafferty, F. W. *J. Am. Soc. Mass Spectrom.* **1995**, *6*, 229−233.
(44) Joenvaara, S.; Ritamo, I.; Peltoniemi, H.; Renkonen, R. *Glycobiology* **2008**, *18*, 339−349.
(45) An, H. J.; Tillinghast, J. S.; Woodruff, D. L.; Rocke, D. M.; Lebrilla, C. B. *J. Proteome Res.* **2006**, *5*, 2800−2808.
(46) Kaji, H.; Yamauchi, Y.; Takahashi, N.; Isobe, T. *Nat. Protoc.* **2006**, *1*, 3019−27.
(47) Grass, J.; Pabst, M.; Chang, M.; Wozny, M.; Altmann, F. *Anal. Bioanal. Chem.* **2011**, *400*, 2427−2438.
(48) Chen, R.; et al. *J. Proteome Res.* **2009**, *8*, 651−661.
(49) Hua, S.; An, H. J. *BMB Rep.* **2012**, *45*, 323−30.
(50) Hua, S.; et al. *Anal. Bioanal. Chem.* **2012**, *403*, 1291−1302.
(51) An, H. J.; Peavy, T. R.; Hedrick, J. L.; Lebrilla, C. B. *Anal. Chem.* **2003**, *75*, 5628−5637.
(52) Nwosu, C. C.; et al. *J. Proteome Res.* **2011**, *10*, 2612−24.
(53) Seipert, R. R.; Dodds, E. D.; Lebrilla, C. B. *J. Proteome Res.* **2008**, *8*, 493−501.
(54) Clowers, B. H.; Dodds, E. D.; Seipert, R. R.; Lebrilla, C. B. *J. Proteome Res.* **2007**, *6*, 4032−4040.
(55) Froehlich, J. W.; et al. *Anal. Chem.* **2011**, *83*, 5541−5547.
(56) Christiansen, M. N.; Kolarich, D.; Nevalainen, H.; Packer, N. H.; Jensen, P. H. *Anal. Chem.* **2010**, *82*, 3500−3509.
(57) Williams, T. I.; et al. *J. Mass Spectrom.* **2008**, *43*, 1215−1223.
(58) Elias, J. E.; Gygi, S. P. *Methods Mol. Biol.* **2010**, *604*, 55−71.
(59) Elias, J. E.; Gygi, S. P. *Nat. Methods* **2007**, *4*, 207−214.
(60) Tabb, D. L.; Fernando, C. G.; Chambers, M. C. *J. Proteome Res.* **2007**, *6*, 654−661.
(61) Ritchie, M. A.; Gill, A. C.; Deery, M. J.; Lilley, K. *J. Am. Soc. Mass Spectrom.* **2002**, *13*, 1065−77.
(62) Harazono, A.; et al. *J. Chromatogr., B: Anal. Technol. Biomed. Life Sci.* **2008**, *869*, 20−30.
(63) Harazono, A.; Kawasaki, N.; Kawanishi, T.; Hayakawa, T. *Glycobiology* **2005**, *15*, 447−462.

(64) Gupta, N.; Bandeira, N.; Keich, U.; Pevzner, P. *J. Am. Soc. Mass Spectrom.* **2011**, *22*, 1111−1120.
(65) Bern, M.; Kil, Y. J. *J. Proteome Res.* **2011**, *10*, 2123−2127.
(66) Nesvizhskii, A. I.; Vitek, O.; Aebersold, R. *Nat. Methods* **2007**, *4*, 787−797.
(67) Computer Software Reviews. *J. Am. Chem. Soc.* **1992**, *114*, 7961−7962.
(68) Brosch, M.; Choudhary, J. *Methods Mol. Biol.* **2010**, *604*, 43−53.
(69) Kim, S.; Gupta, N.; Pevzner, P. A. *J. Proteome Res.* **2008**, *7*, 3354−3363.
(70) Eng, J. K.; McCormack, A. L.; Yates, J. R., III *J. Am. Soc. Mass Spectrom.* **1994**, *5*, 976−989.